IOP Conf. Series: Journal of Physics: Conf. Series **1041** (2018) 012013 doi:10.1088/1742-6596/1041/1/012013

Enhanced energy absorption through dissipation in metal clusters

M. Vincendon[1)], P. G. Reinhard[2)], E. Suraud[1,3)]

1) Laboratoire de Physique Théorique, Université P. Sabatier, 118 Rte de Narbonne, F-31062 Toulouse cedex, France
2) Institut für Theoretische Physik II, Universität Erlangen-Nürnberg, Staudstr. 7, D-91058 Erlangen, Germany
3) School of Mathematics and Physics, Queen's University Belfast, Northern Ireland, UK

E-mail: suraud@irsamc.ups-tlse.fr

Abstract. The paper investigates the dissipation in the electronic dynamics of metallic clusters using a theoretical description in terms of time-dependent mean-field theory with an extension to include electron-electron collisions beyond mean field in terms of a relaxation-time approximation (RTA). The topic is demonstrated on two examples: first, the damping of the all-dominant surface plasmon mode in metallic clusters becoming manifest in the spectral width of the mode and in its lifetime (when viewed in the time domain), and second, the influence of dissipation on the energy absorption of the cluster from an external laser field. The example of laser excitation reveals a dramatic enhancement of energy absorption because dissipation suppresses significantly induced photon emission which is else-wise a process limiting energy intake. The enhancement effect becomes the more important the longer the duration of the laser pulse.

1. Introduction

The optical response of metallic clusters and nano-particles is dominated by the Mie surface plasmon [1, 2, 3]. It constitutes the doorway to laser excitations and thus plays the leading role in nearly all dynamical processes [4]. The average position of the Mie surface plasmon which is an ideal collective dipole mode can be rather well described already with simple approaches as a dipole sum-rule estimate [3], dielectric theory [2], or a fluid dynamical model [5]. This suffices for many estimates in the area of clusters or nano-particles. However, the width of the Mie surface plasmon or its detailed spectral distribution is often also important and it carries a great deal of interesting information. The width characterizes the lifetime of a plasmon and can thus be associated with dissipation. In the time domain, dissipation shows up, e.g., in the damping of the dipole signal with a certain relaxation time. It is the aim of this contribution to discuss, from a theoretical perspective, effects of dissipation in the electronic dynamics of metal clusters as observed in optical absorption spectra, in time evolution of multipole moments, and in energy absorption from an intense laser field. A proper description of the plasmon's width or even detailed spectral distribution requires a deeper microscopic modeling than mere dielectric or fluid dynamical theory. We will take as basis of the microscopic description time-dependent density functional theory (TDDFT) [6, 7]. It has been applied successfully in a great variety of fields [8] amongst them also intensely in cluster physics [9]. Although , as we will see,

TDDFT contains already a large part of dissipation, it misses the contributions from two-body collisions. The latter are brought in by the relaxation-time approximation (RTA) which recently had been made applicable to finite electronic systems [10]. We use this RTA to investigate systematically and compare different electronic relaxation processes in small Na clusters taking Na_9^+ and Na_{40} as examples. The theoretical and numerical background is summarized briefly in section 2. Subsection 2.1, in particular, contains an overview of the various dissipation mechanisms in a cluster or molecule where we work out the distinction between one-body and two-body dissipation. The practical examples are presented and discussed in section 3. It starts with a manifestation in the width of the plasmon resonance seen in the frequency domain, continues with an analysis of relaxation times visualized in the time domain, and elaborates extensively on dissipative effects in the energy absorption during laser-driven cluster dynamics.

2. Theoretical framework

2.1. The concept of dissipation

A complete, fully microscopic description of the dynamics of a many-body system shows no dissipation in the sense that it does not loose any information. One may revert all velocities at a certain instant of time and the system evolves back to the initial state. Dissipation comes into play with reduced description and/or reduced observation. A prominent example is the fluid dynamical description of a system. It employs only local density and current as dynamical variables and thus ignores all intrinsic degrees of freedom which, in turn, leads to various sources of friction [11]. A dynamical mean-field theory, as the time-dependent density-functional theory which we will use later on, is a reduced description of a many-body system in terms of single particle (s.p.) wavefunctions $\varphi_\alpha(\mathbf{r}, t)$. As such it is a fully microscopic description and time reversal invariant thus carrying no dissipation (e.g., a pure mean-field state has single particle entropy zero [10, 12]). At that level, dissipation sneaks in with dynamical correlations beyond mean field. However, when looking at a small set of observables, e.g. a couple of multipole moments, one sees dissipation already from dynamical mean-field theory. This is a case of dissipation by reduced observation. In the following, we will discuss mainly the time evolution of the dipole moment and we will investigate particularly the competition between electronic one-body dissipation and two-body dissipation. The relaxation rates which we find here remain typical for the other low multipole moments.

As already mentioned, we will focus on electronic relaxation processes. Before carrying on, we will briefly summarize all relaxation mechanisms which contribute to cluster dynamics and we do that for the actual example of relaxation rates in dipole dynamics, or widths of the dipole resonance respectively:

1) Dipole oscillations are dominated by the Mie surface plasmon resonance which is the doorway for all dipole excitations processes [2].

2) The fastest relaxation process is Landau dissipation, in spectra also coined Landau fragmentation. This is the leading one-body dissipation which emerges from the distribution of the incoming dipole strength over the energetically close 1ph states. This one-body process starts immediately and leads to relaxation rates for Landau damping of typically 5-20 fs. Most of the 1ph states reside in the regime of bound states and the excitation energy remains in the system.

3) A part of the 1ph states has the particle state above the ionization potential (IP). Coupling to these states leads to direct electron emission associated with similar rates of few 10 fs. Energy is carried away by the emitted electron thus cooling the system besides its typical dissipation effect of damping dipole oscillations.

4) Two-body dissipation stems from electron-electron collisions beyond mean field dynamics. It transfers excitation energy from the 1ph channel into higher order intrinsic excitation thus leading to thermalization of the system. The relaxation rate for this two-body process depends

sensitively on excitation energy, or temperature respectively [13]. It is usually somewhat slower than one-body dissipation with rates within 20-100 fs, but may become as fast as one-body dissipation for very energetic processes. All intrinsic excitation remains initially in the bound regime and leads to thermal electron evaporation only much later, at μs time scale.
5) Coupling to ionic motion (phonons) represents a further dissipation channel. This, however, is a slow process at ionic time scale (order of ps). 6) Ionic disorder, mostly of thermal origin, delivers two sources of dissipation. First, disorder has an impact on the electronic s.p. spectra and thus on one-body dissipation. This is a coherent process at the time scale of electronic one-body dissipation, although the thermal fluctuations of ionic structure go very slowly. Second, a laser beam which hits a thermal ensemble of clusters produces a statistical ensemble of slightly different responses which when added up incoherently yield a substantial broadening of the optical response. This broadening depends, of course, strongly on the temperature of the ensemble.

In the following, we will concentrate on electronic relaxation processes 1–4.

2.2. Mean-field and beyond

Structure and dynamics of the valence electrons of the Na cluster are described in fully quantum-mechanical fashion. Starting point is a mean-field description in terms of density functional theory. Dynamics is treated at the level of the Time-Dependent Local-Density Approximation (TDLDA) treated in the real time domain [6, 7]. The actual electronic exchange-correlation energy functional is taken from Perdew and Wang [14]. A correct description of the ionization potentials (IP) is crucial to simulate electron emission properly. Thus we augment (TD)LDA by a Self-Interaction Correction (SIC) approximated by average-density SIC (ADSIC) [15] which yields correct IP for a wide variety of atoms and molecules [16]. The coupling to the ionic cores is mediated by soft local pseudopotentials [17]. As the present study focuses on the interplay of various electronic dissipation mechanisms, we keep the ionic configuration frozen in the dynamical calculations. In practice, the leading contribution from ionic effects to the spectral widths comes from thermal fluctuations of the ions [18, 19]. These overlay the electronic contributions to the width and so would complicate the analysis.

To provide the basis for later extension, we summarize briefly the formalities of mean-field dynamics. The s.p. wavefunctions are determined by the time-dependent Kohn-Sham equations $(\mathrm{i}\partial_t - \hat{h}[\varrho])\varphi_\alpha = 0$ where the Kohn-Sham hamiltonian $\hat{h}$ is an effective one-body operator depending on the actual local density $\varrho(\mathbf{r}, t)$ [20, 6, 7]. Dissipation leads to mixed quantum states and these are most efficiently described by the one-body density operator $\hat{\rho} = \sum_\alpha |\varphi_\alpha\rangle w_\alpha \langle\varphi_\alpha|$ with occupation weights $0 \le w_\alpha \le 1$. The time-dependent Kohn-Sham equation in terms of density operators reads $\mathrm{i}\partial_t\hat{\rho} - [\hat{h}, \hat{\rho}] = 0$. It changes the s.p. wavefunctions in $\hat{\rho}$, but leaves the occupation weights w_α invariant.

Dynamical correlations beyond mean field can deliver substantial contributions to dissipation. We describe them by the relaxation-time approximation (RTA) [21, 13] which had been adapted recently to describe finite electronic systems [10, 12]. The idea is to simulate the electron-electron collisions by a relaxation to the local-instantaneous equilibrium state which is the mean field state with minimal free energy at given local density, local current, and average energy. A fraction of this equilibrium state is mixed with the actual mean-field state according to the relaxation rate which is derived from the in-medium electron-electron cross section at given density and excitation [22, 23]. In most compact form the RTA equations reads

$$\mathrm{i}\partial_t\hat{\rho} - [\hat{h}, \hat{\rho}] = \frac{1}{\tau_{\rm relax}}\left(\hat{\rho} - \hat{\rho}_{\rm eq}[\varrho, \mathbf{j}, E]\right) \quad , \quad \frac{\hbar}{\tau_{\rm relax}} = 0.40\frac{\sigma_{ee}}{r_s^2}\frac{E^*_{\rm intr}}{N} \quad , \tag{1}$$

where $\hat{\rho}_{\rm eq}[\varrho, \mathbf{j}, E]$ is the instantaneous equilibrium for given local density $\varrho(\mathbf{r}, t)$, local current distribution $\mathbf{j}(\mathbf{r}, t)$, and energy E. The ingredients for the relaxation time $\tau_{\rm relax}$ are: $E^*_{\rm intr}$ the

intrinsic (thermal) energy of the system, N the actual number of electrons, σ_{ee} the in-medium electron-electron cross section, and $r_s = (3/(4\pi\overline{\varrho}))^{2/3}$ the Wigner-Seitz radius of the electron cloud [10, 12] computed from the system's average density $\overline{\varrho}$. The expensive part in the RTA equation is the evaluation of the local equilibrium $\hat{\rho}_{\rm eq}[\varrho, \mathbf{j}, E]$. We take advantage of the fact that dissipation is slow as compared to the fastest time scales covered in TDLDA and propagate a couple (50–100) of pure TDLDA steps before carrying out the next evaluation of the r.h.s. in eq. (1). For more details on RTA and its practical handling see [10, 12].

The stationary and time-dependent Kohn-Sham equations for mean field and single-electron wave functions are solved with standard techniques [24, 9]. The Kohn-Sham potential is handled in the Cylindrically Averaged Pseudo-potential Scheme (CAPS) [25, 26] which is an efficient and reliable approximation for metal clusters close to axial symmetry as the present test case Na_9^+ and Na_{40} are. Wavefunctions and fields are thus represented on a 2D cylindrical grid in coordinate space [27]. In our actual calculations, we employ a numerical box extending to 104 a_0 in radial direction and to 208 a_0 along the z-axis with a grid spacing of 0.8 a_0. We use a large set of s.p. states to supply sufficient space for thermalization. It reaches to about 2.7 eV above the chemical potential covering up to 168 s.p. states with maximal azimuthal angular momentum $l_z = 6\hbar$. To solve the (time-dependent) Kohn-Sham equations for the single particle (s.p.) wavefunctions, we use accelerated gradient iterations for the stationary solution [28] and time-splitting for time propagation [29]. The Coulomb field is computed with successive over-relaxation [27]. We use absorbing boundary conditions [24, 30], which gently absorb all outgoing electron flow reaching the boundaries of the grid. This serves to avoid artifact from electrons re-scattered into the active zone around the cluster. Moreover, proper absorption at the boundaries allows to compute all observables related to electron emission [31].

2.3. Excitation mechanisms and observable

The simplest excitation mechanism is an instantaneous dipole boost where each s.p. wavefunction is augmented by the same velocity field as $\phi_\alpha \rightarrow \exp(-\mathrm{i}\, p_0\, \hat{d}_z)\phi_\alpha$ [24, 9]. The boost momentum p_0 regulates its strength. We are characterizing the boost strength in terms of the initial excitation energy $E_0^* = Np_0^2/(2m)$ caused by the boost. The instantaneous dipole boost models to a good approximation the time-dependent Coulomb field at the cluster site for collisions with very fast ion passing by the cluster [32, 31] or extremely short laser pulses.

Most experiments use excitation by laser pulses. In our simulations, the external laser field is described as a classical electro-magnetic wave in the limit of long wavelengths. This augments the Kohn-Sham Hamiltonian by a time-dependent external dipole field $U_{\rm ext}(\mathbf{r}, t) = e^2\mathbf{r}\cdot\mathbf{e}_{\rm z}\, E_0\, \sin(\omega_{\rm las}t) f(t)$ with the temporal envelop $f(t) = \sin^2\left(\pi\frac{t}{T_{\rm pulse}}\right)\theta(t)\theta(T_{\rm pulse}-t)$. The laser parameters are: (linear) polarization $\mathbf{e}_{\rm z}$ here chosen along the symmetry axis, the peak field strength E_0 related to laser intensity as $I_0 \propto E_0^2$, the photon frequency $\omega_{\rm las}$, and the total pulse length $T_{\rm pulse}$. The latter is related to the full width at half maximum (of intensity) as FWHM $\simeq T_{\rm pulse}/3$.

There is great variety of observables which can be computed from TDLDA and RTA. We will use here only two of them, the dipole moment and the energy absorbed from the laser field. We consider, in particular, the dipole moment along the cluster's symmetry axis (z-axis) $D(t) = D_z(t) = \int \mathrm{d}^3r\, z\, \rho_{\rm el}(\mathbf{d}, t)$. This employs the electronic density distribution $\rho_{\rm el}$ which is naturally given in density-functional theory. The dipole moment will be shown as such, i.e. as time evolution $D(t)$, and as its Fourier transform from time to frequency domain which yields the dipole strength distribution $S_D(\omega) \propto \int dt\, e^{\mathrm{i}\omega t} D(t)$ according to the recipes of spectral analysis [33]. The energy absorbed from the electro-magnetic field is computed in standard fashion as $E_{\rm abs}(t) = \int_0^t dt' \int d^3r\, \mathbf{E}(t')\cdot\mathbf{j}(\mathbf{r}, t')$, where $\mathbf{E}$ is the external electrical field and $\mathbf{j}$ the local electronic current.

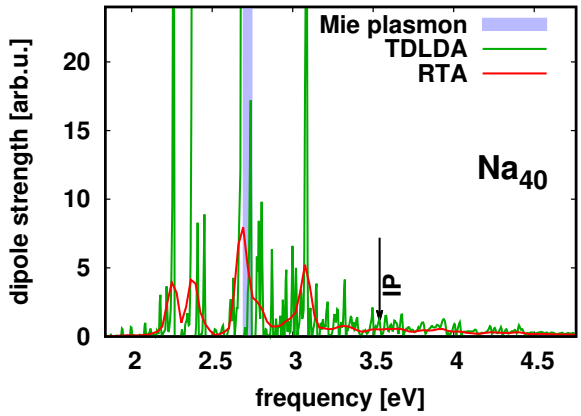

Figure 1: Distribution of dipole strength for Na_{40} computed with TDLDA and RTA in comparison. The strengths were obtained from instantaneous initial dipole boost to excitation energy $E^* = 0.3$ eV with subsequent spectral analysis [33].

3. Results

3.1. Damping mechanisms

We start by visualizing the effect of dissipation processes in spectral strength distribution. Figure 1 shows dipole strength distributions of Na_{40} at three levels of description. The blue shaded area indicates the position of the Mie surface plasmon resonance as estimated in a fluid dynamical approach [5]. This description deals only with collective flow and produces one distinct dipole resonance similar to the estimate with the dipole sum rule [3]. The next deeper level of description is mean-field theory, here in terms of TDLDA. The figure demonstrates nicely how the collective dipole strength of the Mie plasmon is distributed over the many $1ph$ state in the vicinity thus leading to a strongly fragmented distribution, called Landau fragmentation as spectral corollary of Landau damping. The electron emission threshold, the IP, is indicated in the figure. Coupling to ph states above leads to direct electron emission, the dominant energy loss channel. The step to two-body dissipation with RTA changes the spectrum once more. The global strength distribution remains unaffected. But the still spiky structure of the TDLDA spectrum is considerably smoothed thus looking closer to the spectra measured in practice. Note that we used an untypically low excitation energy to stay deep in the regime of linear response. A realistic estimate of width would have to use $E^* \approx 2.7$ eV close to the dominant plasmon resonance and then yield even smoother distributions. A proper spectral smoothing without large-scale reshuffling is the typical and most important effect of two-body correlations also in other areas of physics, see e.g. [34]. The spectrum with RTA still shows more detailed structures than experimental spectra [18]. Note that we are performing our calculations for the ionic ground state of Na_{40} kept frozen at temperature zero. The usually observed smoother spectra stem from incoherent line broadening through thermal fluctuations.

Figure 2 looks at relaxation effects in the time domain for Na_9^+ as test case. In order to avoid interference with time scales of laser excitation, we employ here excitation by an instantaneous dipole boost. All excitation energy is at once deposited on the clusters and after that pure cluster dynamics without external agents follows. This excitation mechanism is free of any time scale and serves to set a well defined initial time. The pure mean-field propagation, marked "mean field", shows a very fast damping of the dipole signal in the initial stages. This is the Landau damping associated with distribution of the dipole strength over the $1ph$ states (see figure 1). But after the first minimum, the dipole signal returns with some amplitude. Mind that the $1ph$ spectrum covers a rather low number of degrees-of-freedom such that corresponding

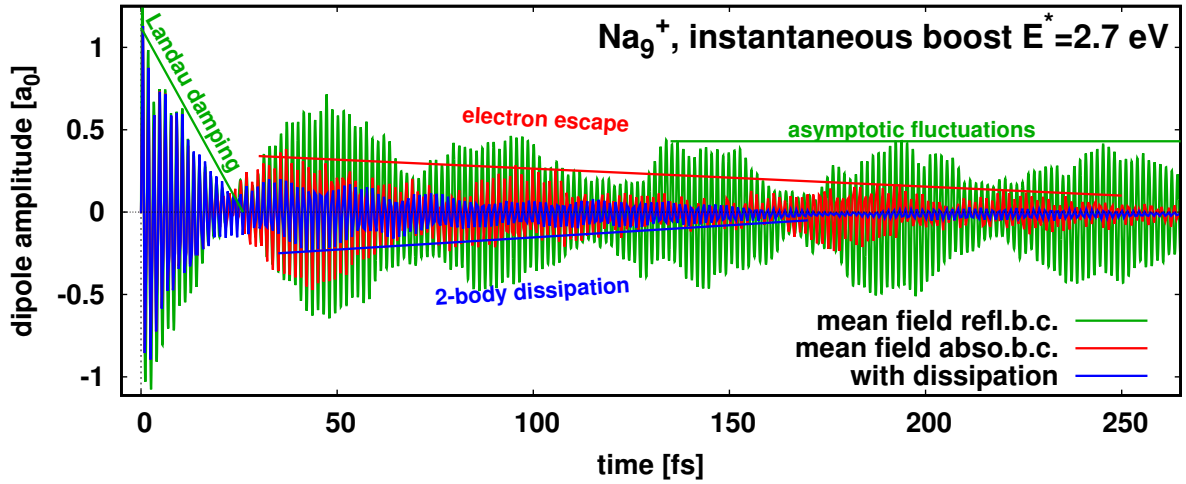

Figure 2: Time evolution of dipole momentum $D_z = \int d^3r\, z\, \rho(\mathbf{r})$ of Na_9^+ after instantaneous dipole excitation. The momentum D_z is the component along symmetry axis of the cluster.

Poincaré recurrence time comes within observation range of the simulation. The signal then shows the typical fluctuations of statistical de-coherence and re-coherence. At long times, the mean-field signal produced with physically appropriate particle emission (look here at "mean field abso.b.c.") shows a slow but steady reduction of recurrent amplitude. This signals the relaxation process from direct electron emission. These electrons are released to the continuum and never come back, thus representing true relaxation. For comparison we show also a results with reflecting boundary conditions. All electrons are forcefully kept in the numerical simulations and so add up to recurrences with undamped amplitude. Finally, we shows the result from RTA now including two-body dissipation. This substantially suppresses the recurrences and lead to a true relaxation with an asymptotically dipole signal. The figure indicates the damping time scales by straight lines associated with the rough envelopes. The hierarchy of relaxation times for the present case has Landau damping as fastest, followed by two-body dissipation, and after that comes relaxation by emission. These relations strongly depend on excitation energy. Here we have chosen $E^* = 2.7$ eV, the energy of a one-plasmon excitation. Processes at multi-plasmon energies lead to significantly faster two-body relaxation and also to faster emission. Note also that we deal here with a positively charged cluster. A neutral cluster, having lower IP, will produce more electron emission leaving less relative weight to two-body dissipation.

3.2. Dissipation versus induced photon emission

A realistic scenario for cluster dynamics is excitation by a laser pulse. The internal relaxation times within the system once excited have been studied above. The question is now which impact dissipation has on the interaction of a system with the laser pulse. A key observable for this is the energy absorbed from the external field. Figure 3 compares the time evolution of absorbed energy for TDLDA and RTA for two laser pulses of different length. The laser frequency is chosen in resonance with the strong Mie plasmon mode. We thus encounter a typical resonant scenario and we spot at first glance that dissipation makes a large difference on energy absorption. Much more energy becomes loaded from the laser field if dissipation is at work. TDLDA and RTA develop much in parallel in the initial stages. The differences develop with the first "oscillation" in $E_{\rm abs}$ which is around 50 fs for the shorter pulse (left panel) and 70 fs for the longer one (right panel). At first glance somewhat surprising, the absorbed energy suddenly turns to decrease which means that the laser field removes energy from the system

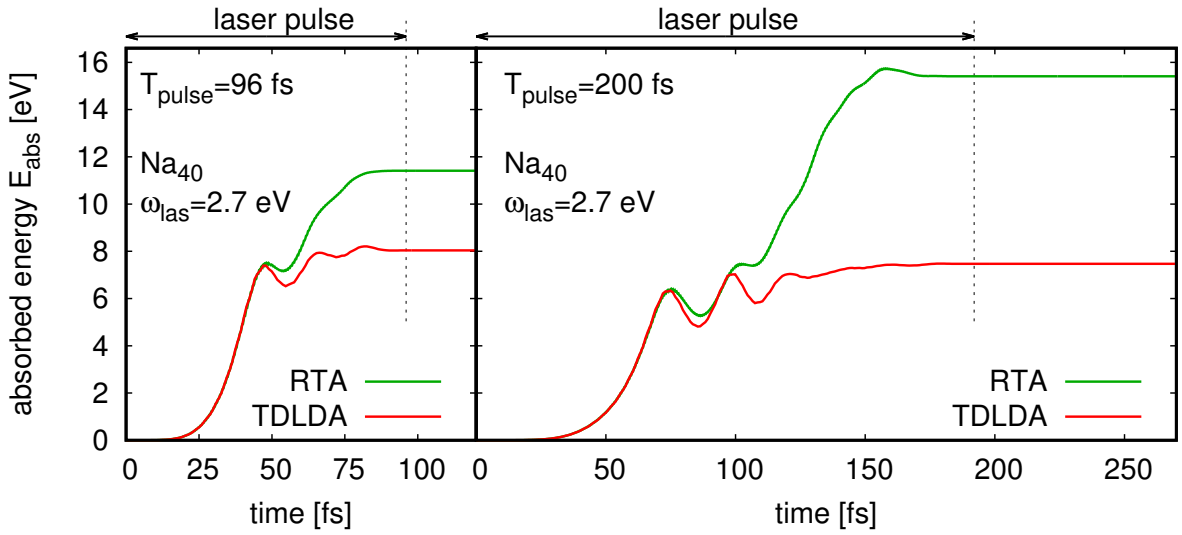

Figure 3: Time evolution of energy $E_{\rm abs}$ absorbed from the laser pulse for the Na_{40} cluster irradiated by a laser with frequency $\omega_{\rm las} = 2.7$ eV (at Mie plasmon resonance), field strength $E_0 = 0.017$ eV/a$_0$ with pulse length $T_{\rm pulse} = 96$ fs or field strength $E_0 = 0.015$ eV/a$_0$ with pulse length $T_{\rm pulse} = 192$ fs. Compared are results from TDLDA and RTA.

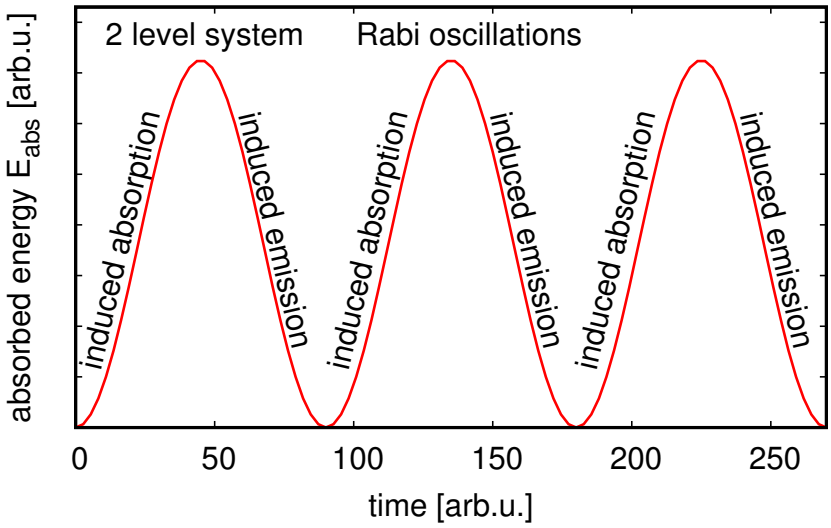

Figure 4: Schematic plot of the time evolution of energy absorption for a coherent photon field coupled to a two-level system.

rather than delivering. This is particularly pronounced for TDLDA whereas RTA suppresses this energy removal and thus allows to swallow more energy from the laser field. This repeats with each oscillation in energy absorption and eventually accumulates to a large difference in total absorbed energy, the larger the longer the pulse.

What we observe here is, in fact, a remnant of Rabi oscillations in a complex electronic system. To recall the principle, we show in figure 4 schematically the time evolution of absorbed energy $E_{\rm abs}$ for the genuine Rabi setup, a mere two-level system coupled to a monochromatic laser field. The $E_{\rm abs}$ undergoes perfect harmonic oscillations which can be explained as changing

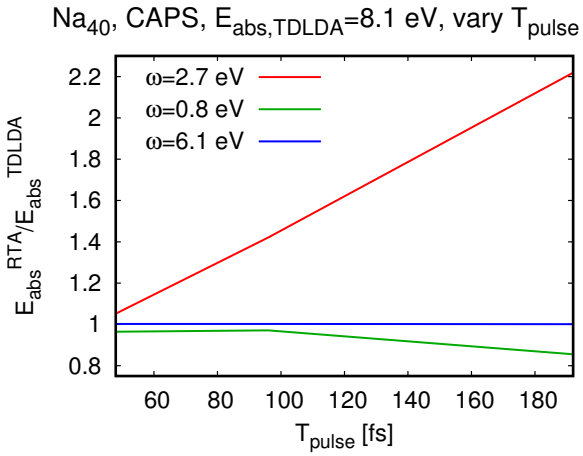

Figure 5: Ratio of final energy absorption with RTA to energy absorption with TDLDA as function of pulse length $T_{\rm pulse}$for a laser pulse with three frequencies as indicated. The field strength, or intensity respectively, had been tuned in each case such that $E_{\rm abs}^{\rm (TDLDA)} = 8.1$ eV for the case of TDLDA.

phases of induced photon absorption and induced emission [35], as indicated in the figure. Both processes, induced absorption and emission are always simultaneously present. But the prevalence of a process changes periodically. As soon as the photon field has sufficiently loaded the two-level system with energy, emission gains over absorption until the energy drops to a level where absorption starts to prevail. The turn to decreasing energy in laser excitation of the Na_9^+ cluster as shown in figure 3 is also caused by this effect that coherent dipole oscillations become sufficiently large to feed induced photon emission. It is, so to say, a remnant of Rabi oscillations in a complex system. It appears because the space of $1ph$ degrees-of-freedom is not large enough to destroy immediately all coherence in the dipole excitation. This changes with dissipation switched on. RTA effectively simulates the coupling to higher configurations ($2ph$, $3ph$, ...) which opens a much larger space of degrees-of-freedom, reduces coherence of the dipole oscillations, and so suppresses induced emission.

As observed in figure 3, the net effect of enhanced energy absorption becomes the larger the longer the pulse. This is demonstrated more systematically in figure 5 showing the enhancement factor for energy absorption with RTA relative to TDLDA as function of pulse length. The trend is obvious and dramatic. It demonstrates for the example of the observable $E_{\rm abs}$ that TDLDA becomes increasingly dubious the longer the simulations. A proper description of long-time behavior in energetic dynamical processes requires to account for dissipative effects beyond TDLDA.

4. Conclusions

We have discussed in this contribution electronic dissipative mechanisms encountered in the course of laser irradiation processes on simple metal clusters. The topic is important for numerous applications, especially in the strongly developing field of plasmonics in nano size systems. We have discussed in detail various mechanisms at work separating explicitly one-body and two body effects. While one-body effects can be analyzed within time dependent mean field theories, two body-effects (electron-electron collisions) require approaches beyond mean field. We used here a Relaxation Time Approach recently developed for finite quantum systems. Comparing RTA with mere mean-field theories, we have shown that these two-body

effects play an important role for energy deposition from the laser into the system. Mean-field dynamics sooner or later hinders further energy absorption because strong coherent dipole oscillations feed enegy loss through induced photon emission. Dissipation, as modeled here by RTA, reduces dipole coherence and so paves the way to considerably enhanced energy absorption. The longer the laser pulse the larger the enhancement factor. This is an important issue which in particular points out the intrinsic limitations of time dependent mean field approaches which might strongly impact numerous applications.

Acknowledgments
This work was supported by the Institut Universitaire de France and the regional computing center Erlangen (RRZE).

[1] Mie G 1908 *Ann. Phys. (Leipzig)* **25** 377
[2] Kreibig U and Vollmer M 1993 *Optical Properties of Metal Clusters* vol 25 (Springer Series in Materials Science)
[3] Brack M 1993 *Rev. Mod. Phys.* **65** 677
[4] Fennel T, , Meiwes-Broer K H, Tiggesbäumker J, Reinhard P G, Dinh P M and Suraud E 2010 *Rev. Mod. Phys.* **82** 1793
[5] Reinhard P G, Genzken O and Brack M 1996 *Ann. Phys. (N.Y.)* **5** 576
[6] Gross E K U and Kohn W 1990 *Adv. Quant. Chem.* **21** 255
[7] Gross E K U, Dobson J F and Petersilka M 1996 *Top. Curr. Chem.* **181** 81
[8] Marques M and Gross E 2004 *Annual Review of Physical Chemistry* **55** 427–455
[9] Reinhard P G and Suraud E 2004 *Introduction to Cluster Dynamics* (New York: Wiley)
[10] Reinhard P G and Suraud E 2015 *Ann. Phys. (N.Y.)* **354** 183
[11] Balescu R 1975 *Equilibrium and Non-Equilibrium Statistical Mechanics* (New York: Wiley)
[12] Vincendon M, Suraud E and Reinhard P G 2017 *Eur. Phys. J. D* **71** 179
[13] Pines D and Nozières P 1966 *The Theory of Quantum Liquids* (New York: W A Benjamin)
[14] Perdew J P and Wang Y 1992 *Phys. Rev. B* **45** 13244
[15] Legrand C, Suraud E and Reinhard P G 2002 *J. Phys. B* **35** 1115
[16] Klüpfel P, Dinh P M, Reinhard P G and Suraud E 2013 *Phys. Rev. A* **88** 052501
[17] Kümmel S, Brack M and Reinhard P G 1999 *Eur. Phys. J. D* **9** 149
[18] Ellert C, Schmidt M, Schmitt C, Reiners T and Haberland H 1995 *Phys. Rev. Lett.* **75** 1731
[19] Montag B and Reinhard P G 1995 *Phys. Rev. B* **51** 14686
[20] Dreizler R M and Gross E K U 1990 *Density Functional Theory: An Approach to the Quantum Many-Body Problem* (Berlin: Springer-Verlag)
[21] Bhatnagar P L, Gross E P and Krock M 511 *Phys. Rev.* **94** 1954
[22] Köhn J, Redmer R, Meiwes-Broer K H and Fennel T 2008 *Phys. Rev. A* **77** 033202
[23] Köhn J, Redmer R and Fennel T 2012 *New J. Phys.* **14** 055011
[24] Calvayrac F, Reinhard P G, Suraud E and Ullrich C A 2000 *Phys. Rep.* **337** 493
[25] Montag B and Reinhard P G 1994 *Phys. Lett. A* **193** 380
[26] Montag B and Reinhard P G 1995 *Z. Phys. D* **33** 265
[27] Davies K T R and Koonin S E 1981 *Phys. Rev.* **C23** 2042–2061
[28] Blum V, Lauritsch G, Maruhn J A and Reinhard P G 1992 *J. Comp. Phys* **100** 364
[29] Feit M D, Fleck J A and Steiger A 1982 *J. Comp. Phys.* **47** 412
[30] Reinhard P G, Stevenson P D, Almehed D, Maruhn J A and Strayer M R 2006 *Phys. Rev. E* **73** 036709
[31] Wopperer P, Dinh P M, Reinhard P G and Suraud E 2015 *Phys. Rep.* **562** 1
[32] Bär M, Jakob B, Reinhard P G and Toepffer C 2006 *Phys. Rev. A* **73** 022719
[33] Calvayrac F, Reinhard P G and Suraud E 1997 *Ann. Phys. (N.Y.)* **255** 125
[34] Tselyaev V, Lyutorovich N, JSpeth, Krewald S and Reinhard P G 2016 *Phys. Rev. C* **94** 034306
[35] Milonni P W and Eberly J H 1988 *Lasers* (New York: Wiley)